16th World Conference on Earthquake Engineering, 16WCEE 2017
Santiago Chile, January 9th to 13th 2017
Paper N° 5003
Registration Code: S-A1479327300

M_w7.8 MUISNE, ECUADOR 4/16/16 EARTHQUAKE OBSERVATIONS: GEOPHYSICAL CLUSTERING, INTENSITY MAPPING, TSUNAMI

T. Toulkeridis[1], K. Chunga[2], W. Rentería[3], F. Rodriguez[4], F. Mato[5], S. Nikolaou[6], N. Antonaki[7], G. Diaz-Fanas[7], M. Cruz D´Howitt[8], D. Besenzon[9], H. Ruiz[10], H. Parra[11], and X. Vera-Grunauer[12]

[(1)] *Researcher-Lecturer, Universidad de las Fuerzas Armadas ESPE, Sangolquí, Ecuador, ttoulkeridis@espe.edu.ec*
[(2)] *Researcher-Lecturer, Universidad Estatal de la Península de Santa Elena, Facultad de Ciencias de la Ingeniería, Santa Elena, Ecuador, kervin.chunga@gmail.com*
[(3)] *Director-Researcher, Instituto Oceanográfico de la Armada del Ecuador (INOCAR), Guayaquil, Ecuador, wjrenteria@gmail.com*
[(4)] *Researcher-Lecturer, Universidad de las Fuerzas Armadas ESPE, Sangolquí, Pontificia Universidad Católica del Ecuador (PUCE), Facultad de Economía, Quito, Ecuadorffrodriguez3@espe.edu.ec*
[(5)] *Researcher, Universidad de las Fuerzas Armadas ESPE, Sangolquí, Ecuador, fjmato@gmail.com*
[(6)] *Principal, Multi-Hazards & Geotechnical Engineering, WSP|Parsons Brinckerhoff, USA, nikolaous@pbworld.com*
[(7)] *Geotechnical Engineer, WSP|Parsons Brinckerhoff, USA, antonakin@pbworld.com, diaz-fanas@pbworld.com*
[(8)] *Researcher-Lecturer, Universidad de las Fuerzas Armadas ESPE, Sangolquí, Ecuador, macruz@espe.edu.ec*
[(9)] *Lecturer, Universidad Estatal de la Península de Santa Elena, Facultad de Ciencias de la Ingeniería, Ecuador, esenzon@espol.edu.ec*
[(10)] *Vice-Dean, Universidad de las Fuerzas Armadas ESPE, Sangolquí, Ecuador, hdruiz@espe.edu.ec*
[(11)] *Head of Department, Universidad de las Fuerzas Armadas ESPE, Sangolquí, Ecuador, haparra@espe.edu.ec*
[(12)] *Head of Instituto de Ingeniería, Universidad Católica Santiago de Guayaquil, Geoestudios, Ecuador, xvg@geoestudios.com.ec*

Abstract

This paper presents our evaluation of the geological and geoseismic aspects and tsunami responsible for considerable damage and 663 deaths of the M_w7.8 Muisne earthquake in Ecuador on April 16th 2016. The seismic event sent tens of thousands to refugee camps and affected some two million persons directly, mostly in the coastal area south of the epicenter. Due to large population movement to the Ecuadorian costs in the last decades, high economical losses occurred due to structural damage to almost 30,000 properties, including family houses, but also due to interruption and damage to infrastructure that served main sources of income from fishing, tourism and other industries. Within three days of the main event, field data were collected and a geological survey was performed and provided input for the evaluation of the maximum macroseismic intensities and the predominant geomorphological features. Data on 290 sampling stations on earthquake-induced (coseismic) ground effects were documented and used to reconstruct a geological isoseismal map. Combining the compiled and recorded coseismic field data of higher macroseismic intensities, we developed an intensity map applying the methodology and definitions of the ESI 2007 scale. We also evaluated the distribution and intensities of the aftershocks that demonstrated spatial-temporal affinities. Geotechnical observations of embankment and port behavior following potential development of soil liquefaction and associated loss of strength are discussed based on the GEER-ATC reconnaissance mission in Ecuador [1]. Documentation on the tsunami that followed the main event [2], although less intense and less destructive from historic and expected tsunamis in the region is presented. Closing thoughts on the needs for rebuild towards resilience for future earthquakes and other natural hazards are briefly discussed.

Keywords: Earthquake; tsunami; liquefaction; subduction; Ecuador

1. Introduction

The deadliest natural hazard based on death toll is earthquakes combined with their secondary effects such as tsunamis [3]. The recurrence of seismic events has been studied extensively by researchers (e.g., [4]). Earthquakes can generate tsunamis, either being in or close to masses of water, like lakes, seas or oceans, or through landslides or other types of massive mass movements or failures [5]. There is at least a dozen of known earthquakes and subsequent tsunamis that have claimed more than 100,000 lives. Among these, two single events in China caused more than 700,000 human losses [6], and the 2004 seismically-induced tsunami claimed some 280,000 lives in Indonesia and neighboring countries [7].

In Ecuador, around one dozen tsunamis have been generated during the past two centuries, close-by or above the Colombian-Ecuadorian trench within the existing geodynamic setting [8]. Recent bathymetric mapping detected submarine landslide scars of a steep-sided fracture zone named "Fracture Zone of Yaquina" (FZY) shown on Fig. 1, which is certainly capable of generating tsunamis [9]. The M_w7.8 earthquake of April 16th, 2016 caused hundreds of deaths and considerable physical and economical damage, and generated a tsunami detected during its movement along the Ecuadorian shores. This paper presents observations and evaluations of the spatio-temporal distribution of the main event and its aftershocks, the intensity mapping of the main event based on earthquake-induced phenomena, and the generated tsunami.

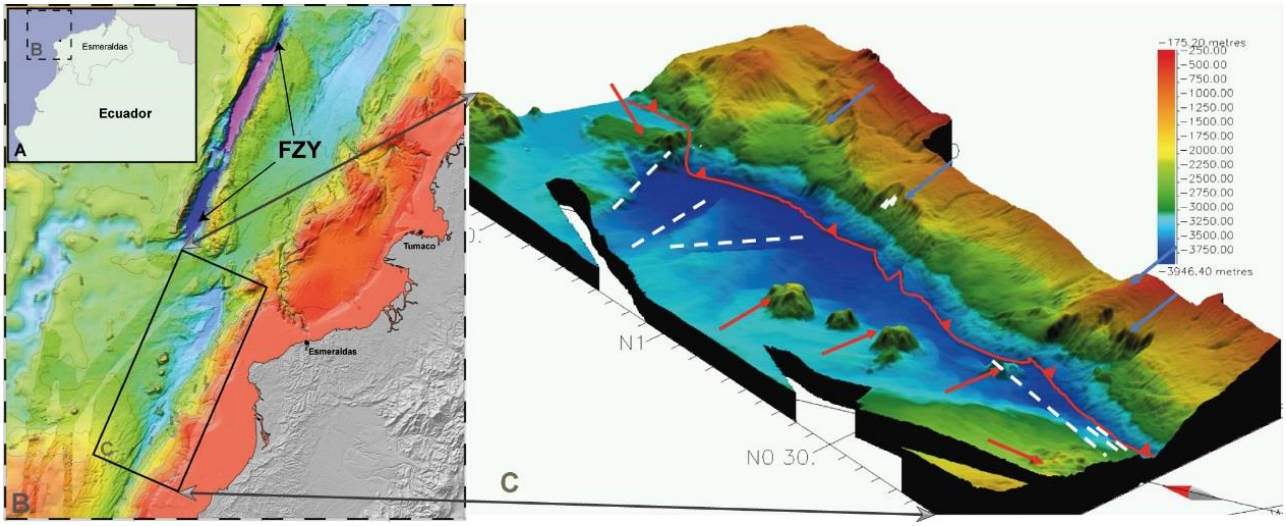

Fig. 1 – (a) Detailed morphology of continental rim of NW Ecuador; (b) Fracture Zone of Yaquina (FZY) extension; (c) geodynamic deformation front between Nazca Oceanic and Caribbean continental plates (red line), active faults at oceanic crust floor (white dashes), seamounts entering the subduction zone (red arrows), and scars of landslides, fissures and submarine debris (blue arrows). Modified from [19].

2. Geodynamic Setting of Ecuador and Seismogenic Origin

Due to its geodynamic situation along the Pacific Rim, the coastal Ecuadorian continental platform is often the target of earthquake activity and subsequent tsunamis ([8], [10]). The active continental margin and associated subduction zone between the oceanic Nazca Plate with the continental South American and Caribbean Plates, both separated by the Guayaquil-Caracas Mega Shear [11] give rise to tsunamis of tectonic, as well as submarine landslide origin ([8], [9]). The main seismic source is the subduction zone, which is about 756 kilometers (km) long, at a distance between 60 and 150 km from the coastline of continental Ecuador.

The volcanic activity and subsequent plate drifting have generated two aseismic volcanic ridges: (i) the Cocos Ridge moving NE above the Cocos Plate and (ii) the Carnegie Ridge moving East above the Nazca Plate [12]. These submarine extinct volcanic ridges are the result of cooling/contraction reactions of magma, as they

slowly sunk below the sea surface due to lack of magma supply, lithospheric movement and strong erosional processes. Over time, these ridges with various microplates, have accreted on the South American continent [13]. Nonetheless, such aseismic ridges may be an obstacle in the oblique subduction, by generating a potential valve of marine quakes within the subduction with earthquakes and tsunamis along the coast [8]. An example is the Carnegie Ridge which collides with the continental margin at ~5 cm/year between latitude 1°N and 2°S [14].

From historic records of the last two centuries, the Ecuadorian shoreline has experienced strong, locally-generated earthquakes and marine quakes, with occasional triggering of tsunamis. The great earthquake of 1906 had an estimated M_w8.8 and 600-km long rupture area [8], with scarce evidence of paleo-tsunami deposits [15] and claimed the lives of approximately 1,500 people in Ecuador and Colombia with unknown overall economic loss. Other earthquakes with subsequent tsunamis along the local subduction zone include the tsunamis of 1942 (M_w7.8), 1958 (M_w7.7), and 1979 (M_w8.2), all within the 1906 rupture area [16]. The 1979 tsunami killed at least 807 persons in Colombia and destroyed about 10,000 homes, destroying power and telephone lines ([17], [18]).

Evaluation of the last marine quakes which generated tsunamis indicate substantial strain accumulation i [8] and suggests that the probability of a major or great earthquake in this margin region is highly likely. Considering that the 1979 earthquake did not release the amount of energy of the 1906 event, there is a high calculated probability of a tsunami similar to that of 1906 in the near future, due to a potential earthquake within the Ecuadorian-Colombian trench. By 2015, this estimated probability of a tsunami strike reached 87% [10] based on historic data of the past 200 years. Such potential tsunami may be even more destructive than past ones if it occurs near high tide [8] and considering the higher risk exposure as the population density has increased along the shorelines as has the infrastructure supporting the major industries of fishing and tourism.

3. The Earthquake of April 16th, 2016

In the late afternoon of Saturday, April 16th, 2015 at 18:58:36 (UTC-05:00) local time, an earthquake with moment magnitude of M_w7.8 impacted coastal Ecuador with epicenter 29 km SSE of the town of Muisne in Esmeraldas province (Lat: 0.353ºN, Lon: 79.925 ºW; [20]) at hypocentral depth of 21 km. The event took the life of 663 people, moved tens of thousands in camps and directly affected the lives of 2 million persons. The event destroyed 70-80% of nearby Pedernales, Jama and Canoa (max macro-seismic intensities of IX-X), and cities within 140-150 km from the epicenter, like Chone, Portoviejo and Manta, which suffered damage to 40-55% of their buildings. Lifelines of electrical power, water supply, and hospitals, schools, private and public facilities, main roads and highways were severely damaged or destroyed. The structural and infrastructure cost was estimated at 3.3 billion USD ([22]; [23]).

The 2016 earthquake has many similarities to the estimated M_w7.8 earthquake of May 14th, 1942, but its tsunami, triggered by a submarine landslide or coseismic deformation, did not have significant impacts. If the epicentral area was within the continental margin and with macroseismic intensity > IX, underwater landslides would be likely [21]. The main event was followed by 84 aftershocks with M_w from 3.8 to 6.8, recorded by USGS and IGEPN until May 20th. The highest magnitudes occurred around the rupture zone with 86% within 10 days of the main shock ([24], [25]).

4. Statistical Evaluation and Geophysical Clustering

A thorough understanding of regional tectonics and modeling of the rupture point to the 2nd plane are essential in explaining how the 2016 earthquake was generated. The earthquake occurred in an area where the subducting Nazca plate under the Caribbean plate slides at 61 mm/year. The focal mechanism was a reverse fault with nodal planes given by the triads (strike, dip, rake) equal to (183°, 75°, 84°) and (26°, 16°, 113°) as reported by USGS [20]. The location and mechanism are consistent with a subduction earthquake interface, sliding over an approximate area 160 km long by 60 km wide. A large number of aftershocks followed for weeks after the main event [26], with 678 events registered within the affected area up to May 20th [27] as shown on Fig. 2a. About 88% of these events were not directly related to the rupture zone [28], as indicated in Fig. 2b [29]. Furthermore, the uncertainty in spatial location of the aftershocks ([26], [27]) reported by IGEPN (Figs. 2a, 3a,b) challenges the study of the subduction process geodynamics (Fig. 4a), masking the existence of 3 distinct seismic clusters (Fig. 4b): (1) Zone 0 (red) at Muisne; (2) Zone 1 (green) at Bahía Caraquez; and (3) Zone 3 (blue) around Manta.

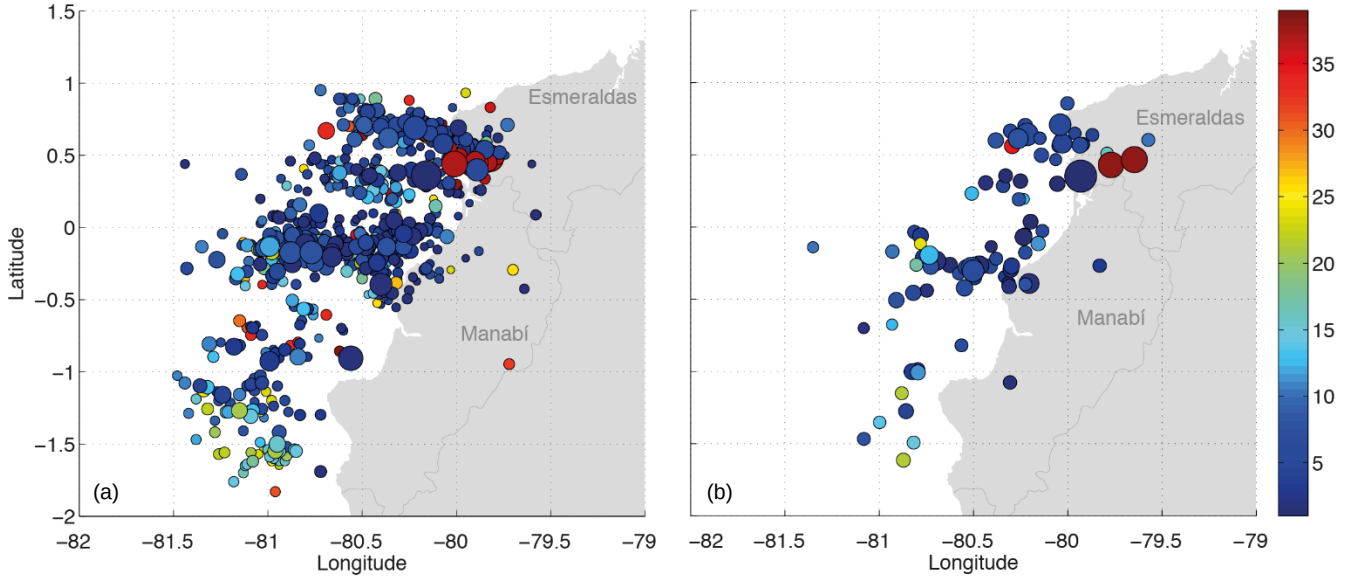

Fig. 2 – Spatio-temporal distribution of the April 16th, 2016 M_w7.8 Muisne earthquake and aftershocks in the affected area [79.5W-81.5W, 2S-1N] by IGEPN (a) and USGS (b) from 4/16 (dark blue) to 5/20 (dark red).

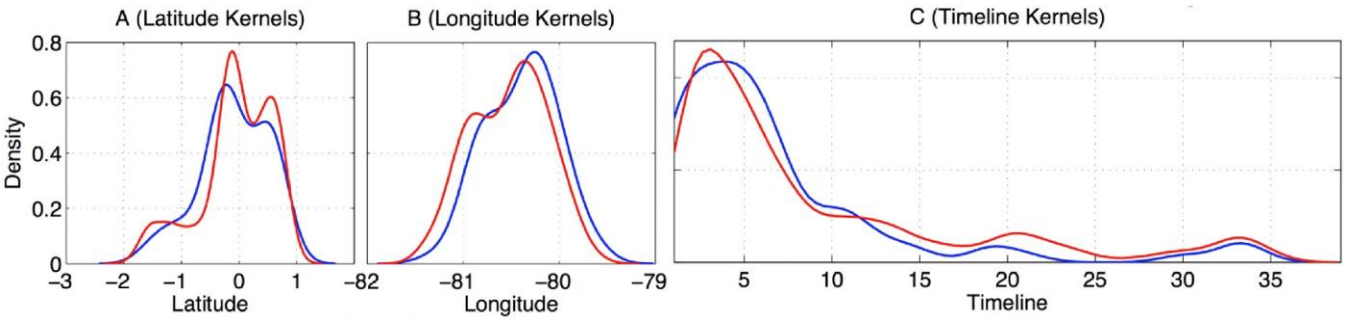

Fig. 3 – Kernels of Lat (A) and Lon (B) of 4/16/16 earthquake and aftershocks in the affected area [79.5W-81.5W, 2S-1N] by IGEPN (red) and USGS (blue); (C) timeline kernels distribution. Observations up to 5/20.

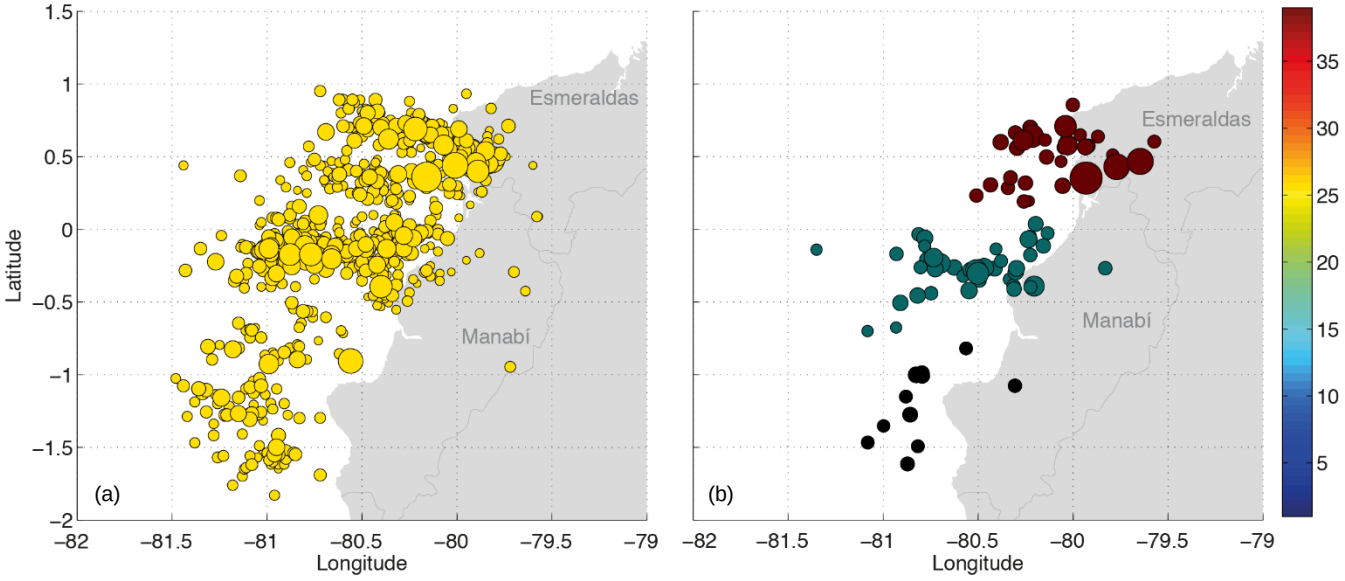

Fig. 4 – (a) IGEPN spatial distribution of 4/16/16 earthquake and aftershocks; (b) geophysical clustering from pre-seismic radiation correlation with spatio-temporal distribution of USGS data [24]. Observations up to 5/20.

The presence of such clusters has been demonstrated [24] by correlating clear pre-seismic radiation with the spatio-temporal distribution of USGS data. The methodology followed allows, with respect to the rupture process: (1) association of seismic events with main points of energy release; (2) geophysical clustering of aftershocks; and (3) identification of geodynamic relationships between clusters since the main shock.

5. Seismic Hazard Evaluation based on Earthquake-Induced Observations

A geological survey and collection of field data collection were performed within 3 days from the main event [1], providing 290 data points of earthquake-induced (coseismic) effects for evaluating max macroseismic intensities (evaluated using the ESI 2007 scale [21]) and predominant geomorphological features. The latter are important in evaluating site effects documented in Muisne, Pedernales, Jama, Canoeing, Chone, San Isidro, Manta, Portoviejo and Tosagua. Aftershocks of the same seismogenic structure as the main event generated settlements and sinkholes, soil liquefaction with sand ejecta and landslides in Pedernales and Mompiche.

Fig. 5 – (a) Liquefaction evidence from GEER army helicopter flyover of Manabí coast, at Jama; (b) landslide on San Vicente-Canoa road. Source: GEER-ATC Report [1].

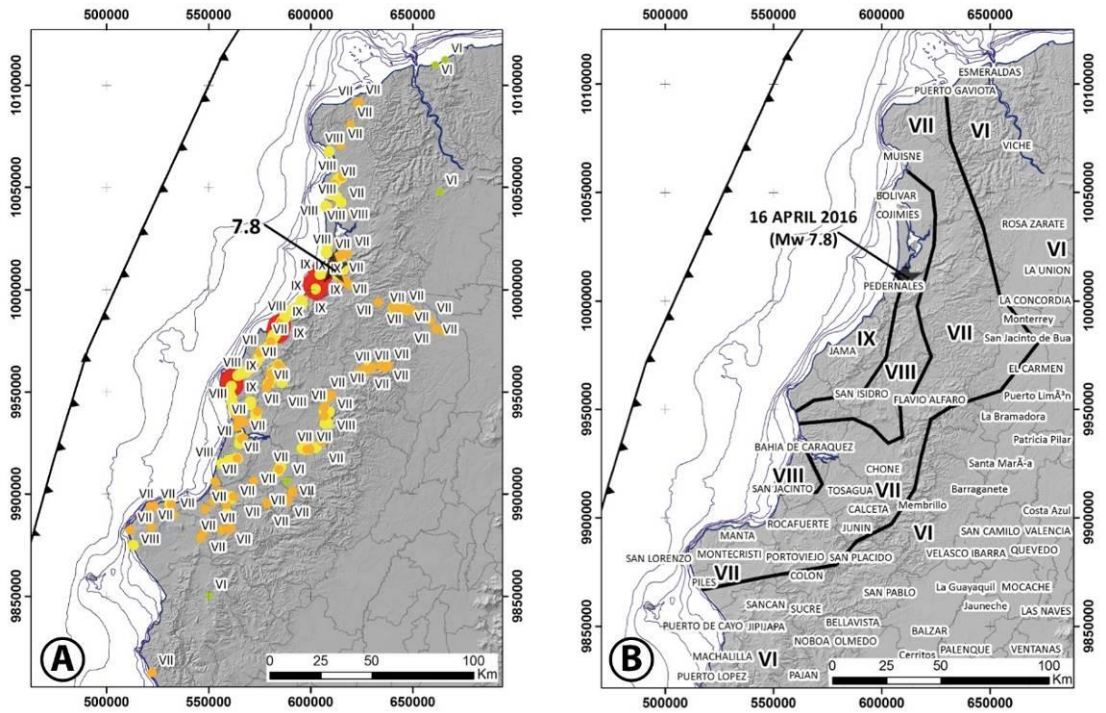

Fig. 6 – (a) Seismic intensities of the main event based on ESI-2007; (b) Zoning of intensity degrees VI-IX [30].

To understand the isoseismal fields of macroseismic intensities the coseismic geological information was compiled in the field based on: (a) landslides of natural and stabilized slopes, (b) cracks in natural field in the supratidal coastal and flood plains, (c) fractures to the main axis of concrete and paved roads, (d) sinkholes and liquefaction in floodplains and areas of paleo-meander, (e) surface faulting with displacements in hilly areas, (f) natural and anthropic subsidence between hills and floodplains, (g) minor tsunami with logs of run-up height < 1 m. Field effects were included for local intensity > VI. The GEER-ATC reconnaissance team provided organized information of earthquake-induced failures [1]. For example, the army helicopter flyover of Manabí coast showed evidence of land settlement and liquefaction in flooded areas with sand ejecta in Jama (Fig. 5a), and landslide at the San Vicente-Canoa local road (Fig. 5b).

Implementing the ESI 2007 scale allowed us to assign intensities based on ground effects in the different geomorphological settings of Manabí and S. Esmeraldas provinces. The sampling stations data were used to reconstruct a geological isoseismal map. With the compiled and field-recorded coseismic data of higher macroseismic intensities, we produced an intensity map by applying the ESI 2007 scale definitions (Fig. 6).

6. Tsunami Evaluation

Worldwide, active continental rims are capable to trigger massive submarine landslides or slope failures, which in turn may generate devastating tsunamis [31]. In such cases, the epicenter does not need to be offshore, but can rather be on the (dry) continental zone.

There is no certainty if the April 16th 2016 tsunami was triggered by a massive submarine landslide or seafloor coseismic deformation. According to the Ecuadorian Oceanographic Institute of the Navy, INOCAR, the tsunami crest arrived at Esmeraldas 6 min after the earthquake. This is a very short travel time from the tsunami landslide scars [32], and for the fault plane of the similar 1942 event [9]. Numerical simulation shows that the tsunami should have travelled > 20 min from its generation zones. When the focal mechanism is well defined, we would update the numerical simulation for seismically-induced tsunami. Nevertheless, a tsunami was triggered, as registered 2 and 3 hours after the earthquake by 32411 and 32413 DART NOAA buoys at the Panama and Peru basins, respectively. Seismic waves propagated over the seabed, affecting the register at the buoys' pressure sensor up to 1 hour after the earthquake (Fig. 7). The tsunami period was approximately 40 min with amplitude of about 1 cm based on observations.

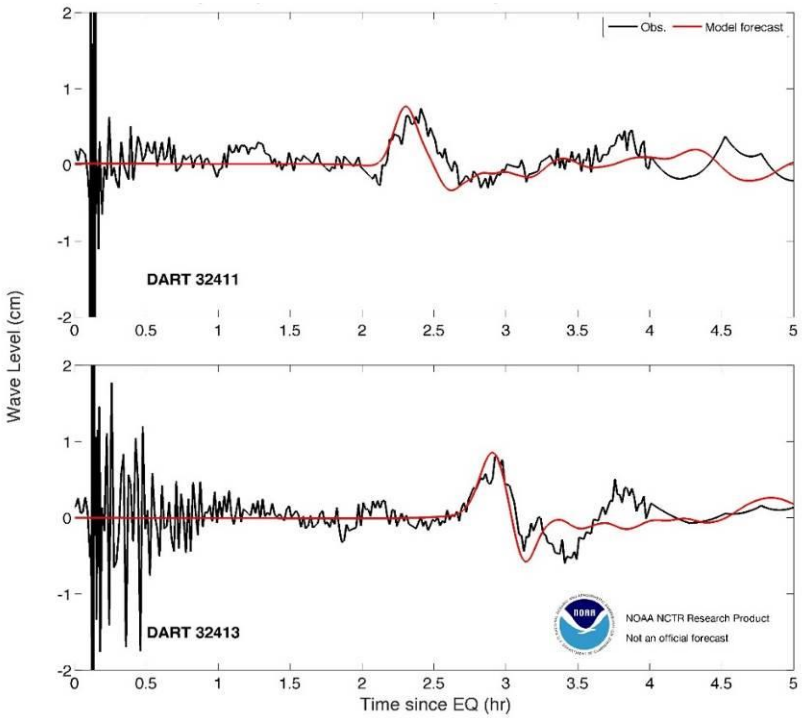

Fig. 7 – Register of oceanic propagation of the tsunami at DART Buoy position. Source: NOAA.

Locally, the tsunami was registered by the INOCAR-DART buoy, which is close to the epicenter, immediately after the earthquake. It has been difficult to differentiate the tsunami signal from the noise produced by the earthquake. However, the perturbation existed after the earthquake time, changing the initial conditions in the calm water level (Fig. 8). INOCAR issued a Tsunami Warning over the entire Ecuadorian coast based on the data from their buoy, which remained in effect 4 hours after the event, considering a potential threat to the shores of the nearby Galapagos Islands. People at the coastal areas reported remarkable changes in seawater levels and also strong rift currents, although the amplitude of the tsunami did not reach a high water level. Fortunately for the coastal communities, the tsunami impact occurred at low tide. This fact appears to be the reason that no inundation occurred and considerable physical effects at the coastlines were absent, which would not be the case under different tide conditions. Some authorities were not concerned that there was a tsunami threat from this event due to the false perception that a tsunami can only be possible if the epicenter was on the ocean side.

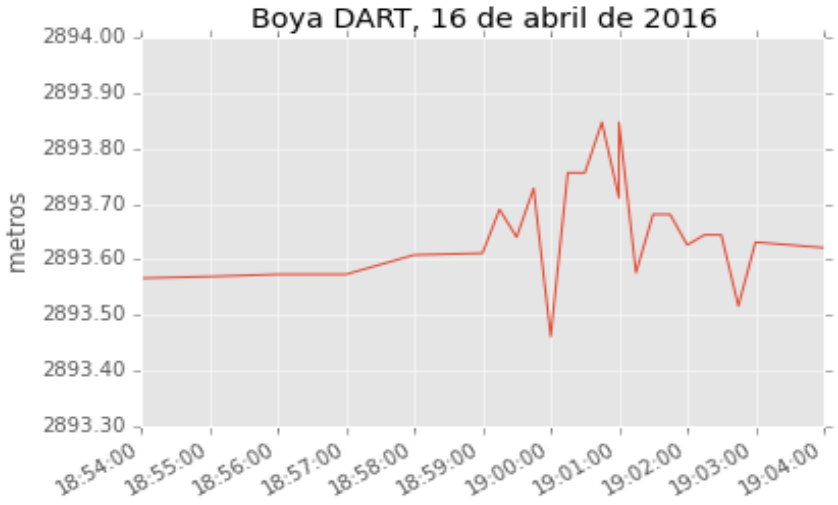

Fig. 8 – Tsunami sea level perturbations. Source: INOCAR.

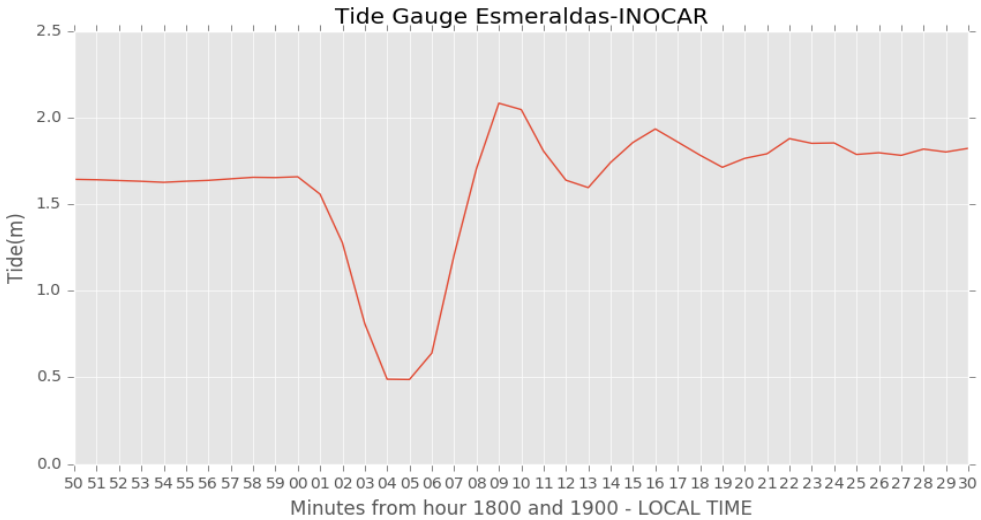

Fig. 9 – INOCAR Mareogram, Esmeraldas Tide Gauge. The tsunami crest wave arrived 6 min after the event.

The Esmeraldas Port registered the tsunami arrival with the receding of the water, started at 19:00. From 19:06 to 19:09, the tide gauge registered the tsunami crest arrival which gives a rate of change in water level of ~50 cm/min. (Fig. 9). Even with arrival at low arrival, the Esmeraldas Port was exposed to strong residual currents. Some small boats and buoys were moved from these anchorage sites due the strong currents (Fig. 10).

Fig. 10 – Small boat and buoys were moved from their anchors due to the tsunami at Esmeraldas port (ECU911).

7. Conclusions

This paper presented observations and evaluations of earthquake-induced effects and associated intensity mapping and triggering of a tsunami following the catastrophic M_w7.8 April 16th 2016, Muisne, Ecuador earthquake. An overall conclusion based on these observations and the estimated loss of this natural disaster is that radical changes in several directions are necessary to rebuild the country targeting resilience goals [33]: (1) improvement in national seismic monitoring system that can produce automated, verified information to scientists and stakeholders with verified epicenter location and magnitude estimates; (2) advanced planning for the response and decision-making chain; (3) implementation of a national research network for early warning i and a national earthquake center; (4) improvement of the local building code to include seismic risk assessment and management; (5) regulations for quality control inspection in implementation of building requirements; (6) development of a clear awareness, preparation, and response plan for the public, including shake-out exercises; (7) creation of a dedicated national emergency unit with all necessary disciplines; (8) development of long-plan resilience goals for infrastructure; and (9) evaluation of national multi-hazard exposure to other natural threats.

Considering the tsunami hazard in particular, more research is needed to clarify if the 2016 tsunami was triggered by an underwater landslide or by the earthquake itself. This research should include bathymetric surveys and multitemporal analysis to identify scars or seafloor deformations. A better estimation of the focal mechanism of the main event is important in order to simulate a synthetic tsunami, to mimic the mareograms obtained at Esmeraldas Port. Moreover, the strong currents generated by the tsunami arrival must be considered by the Maritime Authority for the development of Contingency Plans, since these occurred even though the tsunami did not cause inundation in the coastal basin. Using such simulations with recorded and historical data, a tsunami hazard study should be performed for the vulnerable coastal Ecuador to prepare better for the next one.

8. Acknowledgements

The authors acknowledge the collaboration and exchange of information with the US team of the Geotechnical Extreme Events Reconnaissance (GEER) Association funded by the National Science Foundation (NSF) and the Applied Technology Council (ATC), as listed in [1]. Fernando Mato also acknowledges support by the Prometeo Project of the Ecuadorian Secretariat of Higher Education, Science, Technology & Innovation (SENESCYT).

9. References

[1] Nikolaou, S., Vera-Grunauer, X., Gilsanz, R., eds. (2016): GEER-ATC Earthquake Reconnaissance: April 16 2016, Muisne, Ecuador, *Geotechnical Extreme Events Reconnaissance Association*, Rep. GEER-049, v1. Authors: Alvarado, A., Alzamora, D., Antonaki, N., Arteta, C., Athanasopoulos, A., Bassal, P., Caicedo, A., Casares, B., Davila, D., Diaz, V., Diaz-Fanas, G., Gilsanz, R., González, O., Hernandez, L., Kishida, T., Kokkali, P., López, P., Luque, R., Lyvers, G.M., Maalouf, S., Mezher, J., Miranda, E., Morales, E., Nikolaou, S., O'Rourke, T., Ochoa, I., O'Connor, J.S., Ripalda, F., Rodríguez, L.F., Rollins, K., Stavridis, A., Toulkeridis, T., Vaxevanis, E., Villagrán N., Vera-Grunauer, X., Wood, C., Yepes, H., Yepez, Y. Accessible at geerassociation.org.

[2] Toulkeridis, T., Chunga, K., Rentería, W., Rodriguez, F., Mato, F., Nikolaou, S., Cruz D´Howitt, M., Besenzon, D., Ruiz, H., Parra, H., Vera-Grunauer, X. (2016a). The M_w7.8 earthquake & tsunami of the 16th April 2016 in Ecuador - Seismic evaluation, geological field survey & economic implications, *Science of Tsunami Hazards* (under review).

[3] Holzer, T.L. & Savage, J.C. (2013): Global earthquake fatalities and population. *Earthquake Spectra*, **29** (1), 155-175.

[4] McCaffrey, R. (2008): Global frequency of magnitude 9 earthquakes. *Geology*, **36** (3), 263-266.

[5] Pararas-Carayannis, G. (2014): The Great Tohoku-Oki earthquake and tsunami of March 11, 2011 in Japan: A critical review and evaluation of the tsunami source mechanism. *Pure & Applied Geophysics*, **171** (12), 3257-3278.

[6] Gupta, H.K. et al. (2001): The deadliest intraplate earthquake. *Science*, **291** (5511), 2101-2102.

[7] Ghobarah, A. et al. (2006): The impact of 26 Dec. 2004 earthquake & tsunami. *Eng. Structures*, **28** (2), 312-326.

[8] Pararas-Carayannis, G. (2012). Potential of tsunami generation along the Colombia/Ecuador subduction margin and the Dolores-Guayaquil mega-thrust. *Science of Tsunami Hazards*, **31** (3), 209-230.

[9] Ioualalen, M., Ratzov, G., Collot, J.Y., Sanclemente, E. (2011). The tsunami signature on a submerged promontory: the case study of the Atacames Promontory, Ecuador. *Geophysical Journal International*, 184(2), 680-688.

[10] Rodriguez, F., D'Howitt, M.C., Toulkeridis, T., Salazar, R., Romero, G.R., Moya, V.R., Padilla, O. (2016). Economic evaluation & significance of early relocation vs. complete destruction by a potential tsunami of a coastal city in Ecuador, *Tsunami Society Int.*, **35** (1), 18-33.

[11] Egbue, O. & Kellogg, J. (2010). Pleistocene to present N. Andean "escape". *Tectonophysics* 489, 248-257.

[12] Harpp, K.S. et al. (2003): Genovesa submarine ridge: Manifestation of plume-ridge interaction in N. Galápagos Islands. *Geochemistry, Geophysics, Geosystems*, **4** (9).

[13] Harpp, K.S. & White, W.M. (2001): Tracing a mantle plume: Isotopic and trace element variations of Galápagos seamounts. *Geochemistry, Geophysics, Geosystems*, **2** (6).

[14] Pilger, R.H. (1983): Kinematics of S. American subduction zone from global plate reconstructions. *Geodynamics of the eastern Pacific region, Caribbean and Scotia arcs*: 113-125.

[15] Chunga, K. & Toulkeridis, T. (2014): First evidence of paleo-tsunami deposits of a major historic event in Ecuador. *Tsunami Soc. Int.* 33, 55-69.

[16] Collot, J.Y. et al. (2004): Are rupture zone limits of great subduction earthquakes controlled by upper plate structures? Evidence from multichannel seismic reflection data at N. Ecuador–S. Colombia, *Geophysical Research*, **109** (B11).

[17] Pararas-Carayannis, G. (1980): The earthquake and tsunami of December 12, 1979, in Colombia. *Int. Tsunami Information Center Report*, Abstracted article, Tsunami Newsletter, **XIII** (1).

[18] USGS, US Geologic Survey (2016a): Historic Earthquakes, 1906 Jan. 31st. usgs.gov/earthquakes/1906_01_31.php

[19] Collot, J.-Y. et al. (2010). Vision general de la morfologa submarina del margen convergente de Ecuador-Sur de Colombia. Collot, J.-Y. et al., eds., *CNDM-INOCAR-IRD*, PSE001-09, Guayaquil, Ecuador: 47-74.

[20] USGS (2016b): M7.8-29km SSE of Muisne, Ecuador. earthquake.usgs.gov/earthquakes/eventpage/us20005j32#general

[21] Michetti A.M. et al. (2007): Intensity scale ESI (La Scala di Intensità ESI 2007), L. Guerrieri e. Vittori, eds., *Memorie Descrittive della Carta Geologica d'Italia*, Servizio Geologico d'Italia, APAT, Roma, **74**.

[22] El Telegrafo (2016): eltelegrafo.com.ec/ecuador/manana-se-daran-a-conocer-cifras-oficiales-del-costo-del-terremoto

[23] Senplades (2016): Evaluación de los Costos de Reconstrucción Sismo en Ecuador, Abril 2016. *Secretaría Nacional de Planificación y Desarrollo - Senplades*, Quito, Ecuador, 20 pp.

[24] Toulkeridis et al. (2016b): Real-time radioactive precursor of the April 16, 2016 M_w7.8 earthquake in Ecuador, *Earthquake Spectra* (submitted for review).

[25] Tierra et al. (2016): Evaluation of horizontal and vertical positions obtained from an unmanned aircraft vehicle applied to large scale cartography of infrastructure loss due to the earthquake of April 2016 in Ecuador (submitted)

[26] IGEPN, Instituto Geofísico Escuela Politécnica Nacional (2016a): *Informe Sísmico Nº22*. igepn.edu.ec/n-22-2016

[27] IGEPN (2016b): Earthquake Overview. www.igepn.edu.ec

[28] USGS (2016c): Earthquake Glossary - aftershocks. earthquake.usgs.gov/learn/glossary/?term=aftershocks

[29] USGS (2016d): Earthquake Catalog. earthquake.usgs.gov/earthquakes/search/

[30] Chunga, K. et al. (2016): Areal distribution of ground effects induced by the 2016 M_w7.8 Pedernales earthquake, Ecuador. *88° Congresso della Societa' Geologica Italiana*. S1. Earthquakes & Active Tectonics, Napoli.

[31] Masson, D.G., Harbitz, C.B., Wynn, R.B., Pedersen, G., Løvholt, F. (2006): Submarine landslides. Royal Society of London: Mathematical, *Physical & Engineering Sciences*, **364** (1845), 2009-2039.

[32] Ratzov, G., Collot, J.Y., Sosson, M., Migeon, S. (2010): Mass-transport deposits in the northern Ecuador subduction trench: Result of frontal erosion over multiple seismic cycles. *Earth & Planetary Science Letters*, **296** (1), 89-102.

[33] Nikolaou, S. (2016): The big picture of infrastructure resilience. Keynote on the mini-symposium on infrastructure resilience, *1st Int. Conf. on Natural Hazards & Infrastructure: Protection, Design, Rehabilitation*, Crete, Greece, June